

is the mass of the Li ions surrounding the center. We then assume here that the half-widths of the $n=1$ trapped excitons in the rare-gas solids are determined by the product of a "local mode" factor proportional to the rms displacement of the impurity, and by a "neighbor" factor which is determined essentially by the neighbors of the impurity according to the following relation:

$$W_{ih} \propto M_h^{-1/4}(\text{neighbors}) \times M_h^{-1/4} M_i^{-1/4}(\text{local}). \quad (8)$$

This is just like Eq. (2), the empirical relation for the $n=1$ doublets. A dependence of the linewidth upon the mass of the impurity has been observed also in solid Ar containing hydrogen and deuterium impurities¹¹ and in the U band of alkali halides containing H^- or D^- ions.¹² The $n=2$ states obey Eq. (3) rather than (2); we do not know whether or not the mass of the

impurity enters Eq. (3) because these lines have been observed only in the Xe-doped rare-gas solids. (The Kr-doped samples show only the $n=1$ doublet which lies close to the absorption edges of the neon and argon hosts.) Because of the difference between Eq. (2) and (3) it appears that the interaction of the lattice vibrations with the $n=1$ and $n=2$ excitons is different. This assumption is supported also by the fact that the wave functions of the $n=1$ states are confined to within the unit cell contrary to the $n=2$ states which extend over a larger volume of the crystal.^{1,2}

Experiments on photoconductivity and luminescence, now in progress, are expected to yield more detailed information on the electronic and vibrational states of the rare-gas solids.

ACKNOWLEDGMENTS

The author wishes to express his gratitude to D. L. Dexter, R. S. Knox, and K. J. Teegarden for many helpful conversations.

¹¹ G. Baldini, Phys. Rev. **136**, A248 (1964).

¹² G. Baldini (to be published).

Resistivity of Solid and Liquid Sodium*

MICHAEL P. GREENE AND WALTER KOHN

Department of Physics, University of California at San Diego, La Jolla, California

(Received 10 August 1964)

This paper reports a theoretical study of the resistivity of solid and liquid sodium. It utilizes inelastic neutron scattering data to obtain the required information about the dynamics of the ions. The electron-phonon interaction is characterized by phase-shifts η_i , two of which are used as adjustable parameters. Although the calculation is believed to incorporate accurately many-body effects, umklapp processes, time-dependent effects, etc. agreement with experiment is disappointing. The calculated resistivity exceeds the experimentally measured values by a factor of the order of 2 at low temperatures, and above the melting point there are again discrepancies of this order. No convincing explanation of these disagreements has been found.

I. INTRODUCTION

ONE of the basic tasks of solid-state theory has been to account for the electrical resistivity of simple monovalent metals. The qualitative features of the resistivity of the solid phase, both at very low and at higher temperatures were first theoretically accounted for by Bloch.¹ The next most important landmark was a calculation by Bardeen² who, starting from first principles, was able to give a good quantitative description of the resistivity of sodium and other monovalent solid metals in the high-temperature region. Since then many other calculations on solid metals have been carried out, notably the work of Ziman³ and Bailyn.⁴

A qualitative theory for liquid metals has also been developed by Ziman.⁵

The present work was motivated by the realization that for both solid and liquid sodium experimental data and theoretical methods were available which should enable one to eliminate, within a few percent, all the uncertainties which were known to have been present in past calculations. These included uncertainties about:

- (1) The dynamics of the ions.
- (2) The ion-electron interaction, including many-body effects.
- (3) The validity of the Boltzmann equation.
- (4) The handling of umklapp processes.

For these reasons, good agreement over a wide temperature range was expected.

* Supported in part by the U. S. Office of Naval Research.

¹ F. Bloch, Z. Physik. **52**, 555 (1928).

² J. Bardeen, Phys. Rev. **52**, 688 (1937).

³ J. Ziman, Proc. Roy. Soc. (London) **A226**, 436 (1954).

⁴ M. Bailyn, Phys. Rev. **120**, 381 (1960).

⁵ J. Ziman, Phil. Mag. **6**, 1013 (1961).

In fact, however, this quantitative confrontation of theory with experiment revealed major discrepancies.

(1) At low temperatures the calculated resistivity is substantially too high, about a factor of 2 at 40°K, and a factor of 2.7 at 4.2°K.^{6,7}

(2) In passing through the melting point ($T_m = 371^\circ\text{K}$) the experimental resistivity increases by a factor of 1.5 while the theory gives a factor of about 2.5.

(3) Between $T = T_m$ and $T = 598^\circ\text{K}$, the experimental resistivity increases a little more than linearly with the temperature, by a factor 1.9, while the theory gives a factor 1.3.

We have at present no explanation for these discrepancies, which we consider to be highly disturbing.

Our calculational procedure is briefly the following. We describe the effect of the ions on the conduction electrons by a sum of scattered waves, each centered about the position of an ion. Since it turns out that under all circumstances considered the total scattered amplitude is very small, multiple scattering need not be considered and the standard Boltzmann theory is adequate. The scattering amplitude can be described by a set of phase shifts obeying the Friedel sum rule, a point of view which takes all many-body effects into

account,^{8,9} and it is shown that only two phase shifts are free parameters. It was hoped (in vain) that the entire resistance versus temperature curve could be fitted in terms of these parameters.

The necessary information about the dynamics of the ions is completely contained in the space- and time-dependent pair correlation function, whose Fourier transform $S(\mathbf{k}, \omega)$ can be directly measured by inelastic neutron scattering. In fact, for the solid phase, we calculated $S(\mathbf{k}, \omega)$ from the observed phonon dispersion curves, while for the liquid phase we used directly the results of neutron diffraction experiments.

Effects of recoil, Umklapp processes, etc., are completely included in the general formulation which we used. We have also allowed for more complex electron distribution functions than the usual one ($\sim \mathbf{k} \cdot \mathbf{E}$), but they do not significantly alter the results.

II. GENERAL FORMULATION

In the weak scattering approximation the scattering cross section can be factored into a part depending on the positions and motions of the ions and a part depending on the scattering amplitude from a single ion.¹⁰ A variational calculation of the resistivity then gives (see Appendix)

$$\rho = \frac{(1/32\pi^5 \hbar^2 k T) \iint (d^2 S_{\mathbf{k}}/v_{\mathbf{k}})(d^2 S_{\mathbf{k}'}/v_{\mathbf{k}'}) \{\phi_{\mathbf{k}} - \phi_{\mathbf{k}'}\}^2 |f(\mathbf{q})|^2 \int d\omega S(\mathbf{q}, \omega) \omega / (1 - e^{-\beta\omega})}{\left[\int e v_{\mathbf{k}} \phi_{\mathbf{k}} (\partial f_{\mathbf{k}} / \partial E_{\mathbf{k}}) d^3 k \right]^2}, \quad (2.1)$$

where $\beta = \hbar/kT$.

The two surface integrals are taken over the Fermi surface. \mathbf{k} and \mathbf{k}' are the wave vectors of the initial and final electron states, $\mathbf{q} = \mathbf{k}' - \mathbf{k}$, and $f(\mathbf{q})$ is the appropriate scattering amplitude associated with each ion. $\phi_{\mathbf{k}}$ is the trial function for the perturbed electron distribution, assumed to have the correct cubic symmetry. $v_{\mathbf{k}}$ is the velocity of the electron in state \mathbf{k} . $S(\mathbf{k}, \omega)$ is the dynamical structure factor introduced by Van Hove,¹⁰ who showed how to obtain it from neutron diffraction experiments, and is the Fourier transform of the time-dependent pair correlation function

$$S(\mathbf{q}, \omega) = (1/2\pi N) \int dt e^{-i\omega t} \langle \sum_{i,j} e^{-i\mathbf{q} \cdot \mathbf{r}_i(0)} e^{i\mathbf{q} \cdot \mathbf{r}_j(t)} \rangle_T.$$

$\langle \rangle_T$ represents a thermal average at temperature T , $\mathbf{r}_i(t)$ is the position of an ion at time t and N is the number of ions.

The simplest trial function obeying the symmetry requirements is

$$\phi_{\mathbf{k}} = k_z$$

for an electric field in the z direction. Inserting this into (2.1) we find

$$\rho = \frac{3}{16e^2 k_F^4 v_F^2} \int_{q < 2k_F} d^3 q q |f(\mathbf{q})|^2 \mathcal{S}(\mathbf{q}), \quad (2.2)$$

where we have written

$$\mathcal{S}(\mathbf{q}) = \frac{\hbar}{kT} \int d\omega S(\mathbf{q}, \omega) \frac{\omega}{1 - e^{-\beta\omega}}. \quad (2.3)$$

Formula (2.2) has also been obtained by Baym.¹¹ We present a derivation of (2.1) and (2.2) in the Appendix.

Calculation of the resistivity thus involves two independent tasks. We must find an expression for $f(\mathbf{q})$ in the weak-scattering (linear) approximation, and we

⁶ Since sodium undergoes a martensitic transition from a bcc to a mixture of bcc and hcp phases at about 37°K (see Ref. 7), the significance of data below this temperature is somewhat in doubt.

⁷ C. S. Barrett, J. Inst. Metals 84, 43 (1955).

⁸ J. S. Langer, Phys. Rev. 120, 714 (1960).

⁹ J. S. Langer and V. Ambegaokar, Phys. Rev. 121, 1090 (1961).

¹⁰ L. Van Hove, Phys. Rev. 95, 249 (1954).

¹¹ G. Baym, Phys. Rev. 136, A1691 (1964).

must obtain $S(\mathbf{q})$ with the use of neutron-scattering data. $S(\mathbf{q})$ will be discussed in Sec. III and the scattering amplitude in Sec. IV. Finally we shall present and discuss our results in Secs. V, VI, and VII.

III. DYNAMICAL STRUCTURE FACTOR

(a) Solid Phase

For the solid case, $S(\mathbf{q}, \omega)$ is strongly peaked for each \mathbf{q} around one value of ω which represents the normal vibration or phonon frequency for that \mathbf{q} . For sodium, these frequencies are known in the symmetry directions of the lattice from the neutron diffraction results of Woods *et al.*¹² At off-symmetry points and points outside the first Brillouin zone we can find the frequencies and polarizations vectors by using the following standard procedure. We write the displacement of an ion vibrating in a normal mode of wave vector \mathbf{k} as

$$U_i(n) = \xi_i \exp i(\mathbf{k} \cdot \mathbf{R}_n - \omega t), \quad i = 1, 2, 3, \quad (3.1)$$

where \mathbf{R}_n denotes the equilibrium position. The equation of motion for $U_i(n)$ is

$$M \ddot{U}_i(n) = \sum_m \sum_j \phi_{ij}(n, m) U_j(m), \quad (3.2)$$

where M is the ionic mass. $\phi_{ij}(n, m)$ is the force in the i th direction on atom n due to displacement of atom m in the j th direction. With (3.1)

$$-M\omega^2 \xi_i = \sum_m \sum_j \phi_{ij}(n, m) e^{i\mathbf{k} \cdot (\mathbf{R}_m - \mathbf{R}_n)} \xi_j. \quad (3.3)$$

The frequencies ω and polarizations ξ are found by solving the equation

$$(C_{ij} - M\omega^2 \delta_{ij}) \xi_j = 0,$$

where

$$C_{ij} = \sum_m \phi_{ij}(0, m) e^{i\mathbf{k} \cdot (\mathbf{R}_m - \mathbf{R}_0)}. \quad (3.4)$$

In their paper, Woods *et al.* have fitted their data in the symmetry directions with this model, including interactions between ions out to fifth-nearest neighbors, and published the matrices ϕ . Use of these with Eqs. (3.4) reproduces the frequencies within 1% in the symmetry directions and presumably also to good accuracy in other directions.

With this method, normal as well as Umklapp processes are automatically included. The periodicity of the C matrix insures that wave vectors outside the first zone are properly "folded back" to give the correct frequencies and polarization directions.

Once the frequencies and polarizations are known the structure factor can be calculated. Using the harmonic theory of lattice dynamics in the one phonon approximation and the assumption that the phonons are in

¹² A. D. B. Woods, B. N. Brockhouse, R. H. March, A. T. Stewart, and R. Bowers, Phys. Rev. **128**, 1112 (1962).

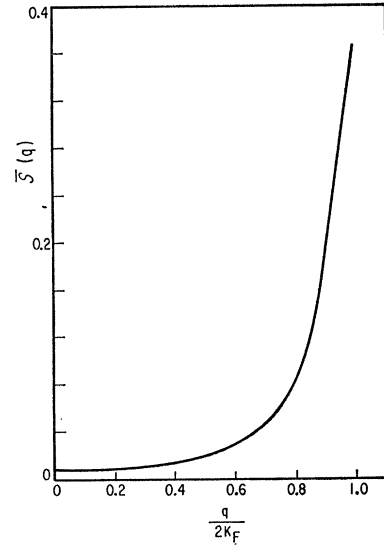
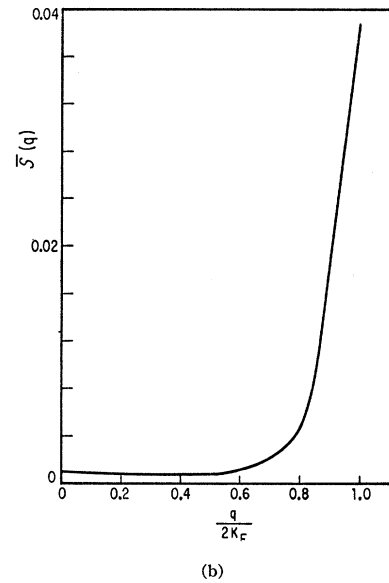


FIG. 1. Structure factor for solid sodium averaged over all directions for fixed q . $\langle S(q) \rangle_{\text{av}}$ versus q . (a) 273°K, (b) 40°K.



thermal equilibrium, we find

$$S(\mathbf{q}, \omega) = \frac{1}{2MN\omega} \sum_p \frac{(\xi_p \cdot \mathbf{q})^2}{e^{\beta\omega} - 1} [\delta(\omega - \omega_{qp}) + \delta(\omega + \omega_{qp})] \quad (3.5)$$

where $p = 1, 2, 3$ are the components of the polarization unit vector ξ . Then

$$S(\mathbf{q}) = \frac{\hbar}{MNkT} \sum_p \frac{(\xi_p \cdot \mathbf{q})^2}{(\exp(\beta\omega_{qp}) - 1)(1 - \exp(-\beta\omega_{qp}))}. \quad (3.6)$$

We define also

$$\langle S(q) \rangle_{\text{av}} = \int (d\Omega_q / 4\pi) S(\mathbf{q}),$$

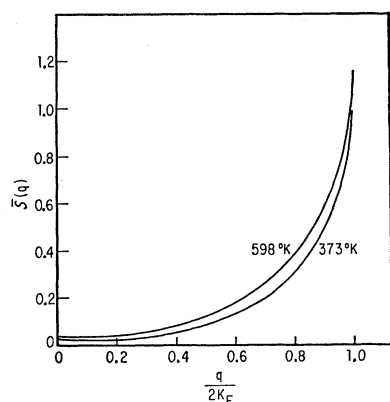


FIG. 2. Structure factor for liquid sodium, $\langle S(q) \rangle_{\text{av}}$ versus q . Note $598/373 = 1.6$ while $\rho(598)/\rho(373) = 1.9$.

an average over all directions for fixed $|\mathbf{q}|$. $\langle S \rangle_{\text{av}}$ is plotted against q in Fig. 1.

In (3.5) and (3.6) only contributions of second order in the ionic displacements have been included. Higher order corrections, including the Debye-Waller factor

$$e^{-2w} = 1 - \langle (\mathbf{q} \cdot \mathbf{U})^2 \rangle_T + \dots,$$

and other multiphonon terms, have been neglected. The correction due to the Debye-Waller factor is about 16% at the melting point; the other terms are of the same order of magnitude and the opposite sign.

(b) Liquid Phase

Above the melting point we can set in good approximation

$$\beta\omega / (1 - e^{-\beta\omega}) = 1 \quad (3.7)$$

and, by Eq. (2.3), read $\langle S(q) \rangle_{\text{av}}$ directly from the energy-integrated neutron-diffraction data.¹³ The validity of approximation (3.7) will be verified in Sec. VII, where the corrections are shown to be less than 2%.

In the long-wavelength limit, $\langle S(q) \rangle_{\text{av}}$ is determined by average thermodynamic properties¹⁴

$$\langle S(0) \rangle_{\text{av}} = n\beta_c kT, \quad (3.8)$$

where $n = N/\Omega$ and β_c is the isothermal compressibility. The published data¹¹ is expressed with forward scattering amplitude set equal to zero; hence we must add in the proper contribution from (3.8). This correction raises the resistivity by only a few percent.¹⁵ $\langle S(q) \rangle_{\text{av}}$ for liquid sodium is pictured in Fig. 2.

IV. SCATTERING AMPLITUDE

The basic assumption underlying this calculation is that the scattering from the sum of all the centers is weak. Then we may neglect multiple scattering, use Van Hove's formalism to separate the cross section into

¹³ N. Gingrich and L. Heaton, *J. Chem. Phys.* **34**, 873 (1961).

¹⁴ A. Guinier and G. Fournet, *Small Angle Scattering of X-Rays* (John Wiley & Sons, Inc., New York, 1955).

¹⁵ The fact that this term has a linear dependence on T cannot be used to infer a linear dependence for the resistivity.

the product $|f(\mathbf{q})|^2 S(\mathbf{q}, \omega)$, and express the scattering amplitude from one center, $f(\mathbf{q})$, in a form linear in the phase shifts. We shall refer to this as the weak scattering approximation to distinguish it from the usual form of the Born approximation. We deal directly with scattered waves originating from the positions of the ions, which add coherently to give a total scattered wave small compared with the incident wave. With this picture we can refer to the work of Kohn and Luttinger¹⁶ who have shown that the usual Boltzmann transport equation holds whenever the scattering can be described in this approximation.

We shall now show that the total cross section is in fact small. Let us assume the existence of a transport equation relating mean free path to scattering cross section and compare the free path derived from conductivity data with the lattice spacing, about 4.25 Å for sodium. Values of the mean free path at various temperatures are presented in Table I. Over the entire temperature range studied, the mean free path is many times the lattice spacing.

Let us now study the scattering amplitude $f(\mathbf{q})$ associated with a single ion. We start with a system of N electrons and a neutralizing charge background contained in a large box of volume Ω . The charge densities of electrons and background are equal in absolute magnitude and are the same as in sodium.

We modify this system in two steps to obtain a representation of actual metallic sodium. First we insert the sodium ions at the appropriate positions—near the lattice sites for the solid or in a somewhat disordered array for the liquid—and around each ion we remove a Wigner-Seitz sphere of the uniform background. At the same time we allow the electrons to come to equilibrium with this new configuration. Let us denote the scattering amplitude from one of these localized disturbances by $f^{(1)}(\theta)$. We may estimate it by representing the ions by the Prokofjew potential,¹⁷ subtracting the potential of a uniform sphere of positive charge and calculating exactly (not in Born approximation) the scattering phase shifts. We find, neglecting multiples of 2π due to bound states which do not affect the scattering,

$$\eta_0^{(1)} = 0.04, \quad \eta_1^{(1)} = 0.021, \quad \eta_2^{(1)} = 0.0087, \quad \eta_3^{(1)} = 0.00027.$$

Clearly an expression for the scattering amplitude linear

TABLE I. Comparison of mean free path with lattice constant for liquid and solid sodium.

T (°K)	40	200	328	373	598
l (Å°)	8000	530	275	150	78
l/a	1900	125	65	35	18

¹⁶ W. Kohn and J. M. Luttinger, *Phys. Rev.* **108**, 590 (1957).

¹⁷ Quoted in E. P. Wigner and F. Seitz, *Phys. Rev.* **43**, 807 (1933).

in the phase shifts is adequate to describe the scattering from each site.

Next, we must put back the charged spheres and remove the uniform background. Since in all situations considered there is substantial short-range order, these actions cancel to a large extent. We denote the remaining charge density by $\rho_2(\mathbf{r})$. As pictured in Fig. 3, ρ_2 consists of partly positive, partly negative "slivers" of charge. The volume of these slivers is small and they will, of course, be screened by the conduction electrons; hence they will produce a small total scattering amplitude $F_2(\theta)$.

We now wish to show that $F_2(\theta)$ can be expressed as a sum of scattering amplitudes each associated with one of the ions and each expressed in a form linear in the phase shifts. We write the external perturbing potential of the "slivers" mentioned above as

$$H' = \lambda \left[\sum_i V_{\text{WS}}(\mathbf{r} - \mathbf{R}_i) - V_0 \right], \quad (4.1)$$

where $V_{\text{WS}}(\mathbf{r} - \mathbf{R}_i)$ is the electrostatic potential due to a Wigner-Seitz sphere of positive charge, V_0 is the electrostatic potential of the entire uniform positive charge background, and λ is a parameter whose actual value is unity. Because the two terms in parentheses largely cancel one another, the perturbation is in fact very small and hence the scattering amplitude $F_2(\theta)$ may be calculated to first order in λ . From this it follows that we shall obtain the correct answer by calculating the scattering amplitude due to each of the terms in Eq. (4.1) to first order in λ and adding. This is so even though the scattering phase shifts due to an individual term $V_{\text{WS}}(\mathbf{r})$ are by no means very small. When calculated in Born approximation, including screening, they are approximately

$$\begin{aligned} \eta_0^{(2)} &= 0.6, & \eta_1^{(2)} &= 0.2, & \eta_2^{(2)} &= 0.05, \\ \eta_3^{(2)} &= 0.015 & \text{and} & & \eta_4^{(2)} &= 0.002. \end{aligned}$$

Nevertheless the above arguments show that, somewhat paradoxically, we *must* use the Born expression

$$f^{(2)}(\theta) = \sum \frac{(2l+1)}{k} \eta_l^{(2)} P_l(\cos\theta)$$

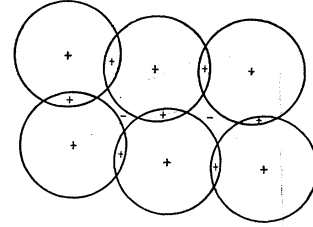
for the scattering amplitude from a Wigner-Seitz sphere.¹⁸

We should still add the scattering amplitude from the uniform background, but since this is entirely in the forward direction it does not contribute to the resistivity and can be dropped.

From these considerations and the numerical estimates of scattering amplitudes we conclude that the resistance may be calculated as though each center gives

¹⁸ The exact expression for $f(\theta)$ in terms of phase shifts [$\eta_l \rightarrow (1/2i)(e^{2i\eta_l} - 1)$] would give different (and hence wrong) results, if contributions from different centers are linearly superposed and cross terms are neglected.

FIG. 3. Charge distribution $\rho_2(\mathbf{r})$.



rise to a scattering amplitude of the form

$$f(\theta) = \sum \frac{(2l+1)}{k} \eta_l P_l(\theta),$$

where the η_l will have values similar to those obtained by adding our numerical estimates for $\eta_l^{(1)}$ and $\eta_l^{(2)}$.

V. EVALUATION OF THE RESISTIVITY

We shall represent the full scattering amplitude $f(\mathbf{q})$ by a set of phase shifts η_l . Examination of the estimates for $f^{(1)}$ and $f^{(2)}$ indicates that we may approximate $f(\mathbf{q})$ with the first four phase shifts.

From Eq. (2.2) we have

$$\rho = \frac{3}{16e^2 k_F^4 v_F^2} \int d^3q |f(\mathbf{q})|^2 \mathcal{S}(\mathbf{q}), \quad (5.1)$$

where

$$f(\mathbf{q}) = -\frac{2\pi\hbar v_F}{k_F^2} \sum_l (2l+1) \eta_l P_l(\mathbf{q}). \quad (5.2)$$

By varying η_3 in our calculations we ascertained that it has small influence on the resistivity; for convenience we set it equal to its calculated value 0.015.

The Friedel sum rule¹⁹ is an exact relation among the phase shifts for scattering from a screened potential. It requires

$$\sum_l (2l+1) \eta_l = \frac{1}{2} \pi Z,$$

where Z is the charge introduced into the electron gas by the localized potential and bound states are neglected. Thus Z is zero for $f^{(1)}$ and one for $f^{(2)}$, and so for f we take Z to be one. The η_l are then not all independent; in particular if we fix η_3 and ignore the higher η_l , then we can use η_0 and η_1 as free parameters to determine the scattering amplitude and fix η_2 by the sum rule. Of course, η_0 and η_1 must be somewhat restrained so that η_2 is not unreasonably large.

Let us write (5.2) in the form

$$f(\mathbf{q}) = \sum_l f_l(\mathbf{q}) \eta_l$$

so that

$$|f(\mathbf{q})|^2 = \sum_{l,l'} f_l(\mathbf{q}) \eta_l \eta_{l'} f_{l'}(\mathbf{q}).$$

¹⁹ J. Friedel, *Advan. Phys.* **3** (1954).

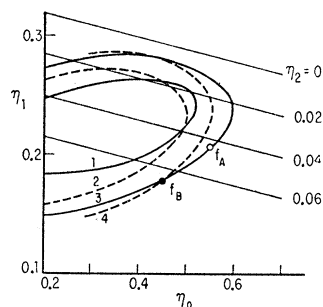


FIG. 4. Phase shifts which provide a fit to the resistivity data, η_1 versus η_0 . $\eta_3 = 0.015$ and $\eta_2 = \pi/2 - (\eta_0 + 3\eta_1 + 7\eta_3)$. (1) Solid sodium, 40°K. (2) Liquid sodium, 373°K. (3) Solid sodium, 200-350°K. (4) Liquid sodium, 598°K.

Inserting in (5.1) we may write for the resistance

$$\rho = \sum_{i,\nu} \rho_{i\nu} \eta_i \eta_\nu, \quad (5.3)$$

with

$$\rho_{i\nu} = \frac{3}{16e^2 k_F^4 v_F^2} \int_{q < 2k_F} d^3 q q f_i(\mathbf{q}) f_\nu(\mathbf{q}) S(\mathbf{q}). \quad (5.4)$$

With our two free parameters, (5.3) represents a conic section in η_0, η_1 space. We find it to be an ellipse.

In the solid phase above 200°K, the experimental resistivity is nearly proportional to T , and examination of (2.3), (3.5), and (5.4) shows that $\rho_{i\nu}$ also varies linearly with T . Values of η_0 and η_1 which fit the observed resistivity lie on one single ellipse for this high-temperature regime. At extremely low temperatures, both experiment and theory should vary as T^5 and this regime should be represented by a different ellipse. At intermediate temperatures we might expect still different ellipses as the weights shifts from short- to long-wavelength phonons. If the theory were a correct description of experiment these curves would intersect at one or more points and there would then exist a set of phase shifts which consistently predicts the resistivity at all temperatures, including the liquid phase. The curves obtained are shown in Fig. 4. From about 200°K to the melting point there is one single ellipse in η_0, η_1 space which provides the observed resistivity. Below 200°K but above the T^5 region, there is a different ellipse for each temperature, all roughly concentric with size decreasing with temperature. The ellipses representing two points in the liquid, 373 and 598°K, are also concentric, with the low-temperature curve within, but are oblique to the ellipses for the solid phase, crossing them at several points. The nonintersection of all these curves indicates that the observed temperature dependence of ρ cannot be fitted with our model over the entire temperature range, nor can a reasonable fit be made over any substantial range below 200°K or above the melting point. This leads us to believe that it is in these two regions that the theory fails.

To study the absolute magnitude of the discrepancy we chose two points from the high-temperature solid ellipse. f_A is close to the estimated value $f^{(1)} + f^{(2)}$ while f_B is near the intersection of the high-temperature solid and high-temperature liquid curves. These are

shown in Fig. 5 as a function of q along with $q^3 f^2$, which is the total weighting factor for $\langle S(\mathbf{q}) \rangle_{av}$ in the integrand of Eq. (2.2). In Fig. 6 we show the results using f_A and f_B as well as experimental values.^{20,21,22}

Concentrating on f_A we see the change in resistance on melting is overestimated by almost a factor of 2; thereafter the calculated resistance of the liquid increases only slightly with temperature while the observed resistance increases faster than linearly. The high temperature solid is described to within 10% except close to the melting point. There vacancy formation and anharmonic effects occur which are not included in the model.²³ At low temperatures, the calculated value at 40°K is too large by nearly a factor 2, and at 4.2°K by a factor of 2.7.²⁴

VI. ROLE OF DIFFERENT GROUPS OF PHONONS AND OF UMKLAPP PROCESSES

In the past the relative contributions of umklapp processes to the thermal part of the electrical resistivity has been a subject of controversy. Early authors neglected them altogether or considered their contribution small. Recently writers have realized their importance, with Bailyn⁴ even suggesting that at low temperatures perhaps normal processes can be neglected.

During the course of our calculations we were able to examine every phonon that contributes to the integral of Eq. (2.2), note whether it takes part in normal or umklapp processes, and compute its relative contribution to the resistivity. We also noted its actual wavelength, i.e., $2\pi/q$ for normal processes and $2\pi/|q-G|$

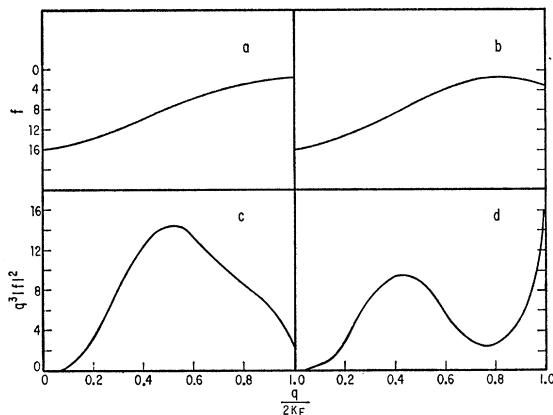


FIG. 5. Scattering amplitudes and weighting factors versus q . (a) f_A . (b) f_B . (c) $q^3 |f_A|^2$. (d) $q^3 |f_B|^2$. Arbitrary units.

²⁰ Dugdale and Gugan, Proc. Roy. Soc. (London) **A254**, 184 (1960).

²¹ Kapelner and Bratton, Pratt and Whitney Technical Report 376, Middleton, Connecticut (unpublished).

²² We also made a calculation for 40°K using another point on the high temperature solid ellipse, $\eta_0 = 0.6, \eta_1 = 0.23$. This gave a value of resistivity about 10% smaller than that for f_A .

²³ We have used a harmonic theory because experimental values for $S(\mathbf{q}, \omega)$ are not available for the solid. For the liquid phase these effects are included.

²⁴ See, however, Ref. 6.

for umklapp processes, where G is a nonzero vector of the reciprocal lattice.

These relative contributions are, of course, highly dependent on the form chosen for the scattering amplitude $f(\mathbf{q})$. Using the estimated function f_A we found that at 273°K umklapp processes contribute 72%, and at 40°K, 79% of the calculated resistivity. Comparison of the curves of Fig. 5 indicate that these fractions would be even greater for the function f_B .

Using f_A , we found that at both 40 and 273°K, over 40% of the resistivity is due to phonons of wavelength between 5.5 and 7 Å and 80% to phonons shorter than 10 Å. The shortest wavelength that contributes is equal to the lattice constant 4.25 Å, which corresponds to the farthest point on the first zone boundary. The electrons' Fermi wavelength is 6.9 Å. $2k_F$ corresponds to 3.5 Å, and so crystal momentum transfers near this magnitude always demand umklapp processes and involve longer phonons. The results are presented in Figs. 7 and 8. The slight dip at 13 Å we ascribe to nothing more than an accident of the method of selection of points for the numerical integration.

VII. DISCUSSION

(1) Effective Mass

In all our work we have tacitly assumed that in the perfect sodium lattice the electrons may be treated as though their E versus \mathbf{k} relationship is the same as for free electrons. We believe that this is a well-justified assumption. De Haas-van Alphen measurements have shown²⁵ that the Fermi surface is spherical to within a fraction of a percent. The mean cyclotron mass is 1.24.²⁶ The effect on the mass of the electron phonon

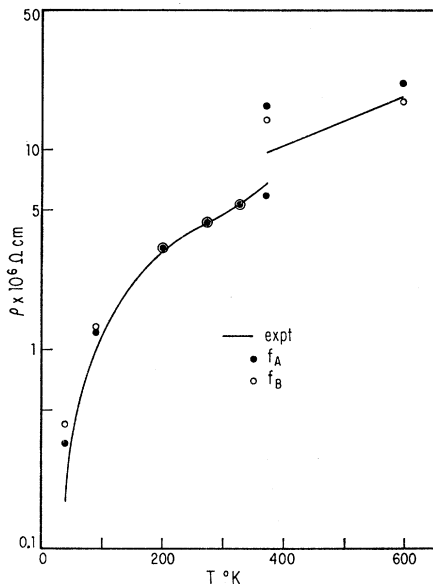


FIG. 6. Resistivity versus temperature for sodium.

²⁵ D. Schoenberg and P. S. Stiles (private communication).

²⁶ C. C. Grimes and A. F. Kip, Phys. Rev. **132**, 1991 (1963).

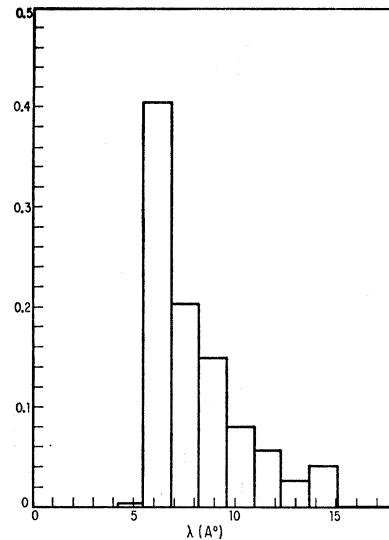


FIG. 7. Fractional contribution to the resistivity of sodium by phonon of wavelength λ . $T=40^\circ\text{K}$.

interaction is estimated to be 33%²⁷ and has been shown not to influence the resistivity in lowest order.²⁸

(2) Low-Temperature Solid

Attacking first the discrepancy at low temperatures we considered two effects which might tend to lower the resistivity from the calculated value.

(i) Anisotropy of the Phonon Spectrum

At low temperatures where only low-frequency phonons are present, an electron moving in certain directions might not find a phonon available from which to scatter. This would cause higher angular harmonics to be present in the perturbed electron distribution. The calculation of Eq. (5.1) included only the simplest trial function with the proper symmetry $\phi = k_z$. (Sondheimer²⁹ has used trial functions of the form k_z^{2n} and found very little contribution from terms with $n \neq 0$.) To take account of the anisotropy of the phonon spectrum some angular freedom is necessary in the electronic trial function.

We considered trial functions of the form

$$\begin{aligned} \phi_1 &= a_{11}z, \\ \phi_2 &= a_{21}z + a_{22}z^3, \\ \phi_3 &= a_{31}z + a_{32}z^3 + a_{33}z^5, \\ \phi_4 &= a_{41}z + a_{42}z^3 + a_{43}z^5 + a_{44}z(x^4 + y^4), \\ \phi_5 &= a_{51}z + a_{52}z^3 + a_{53}z^5 + a_{54}z(x^4 + y^4) + a_{55}zx^2y^2, \end{aligned} \quad (6.1)$$

where $z = k_z/k_F$, etc. We inserted the functions (6.1) into the variational expression (2.1) and minimized with respect to the a 's. The procedure is described in the appendix and results presented in Table II.

²⁷ R. E. Gaumer and C. V. Heer, Phys. Rev. **118**, 955 (1960).

²⁸ S. Nakajima and M. Watabe, Progr. Theoret. Phys. (Kyoto) **29**, 341 (1963).

²⁹ E. H. Sondheimer, Proc. Roy. Soc. (London) **A203**, 75 (1950).

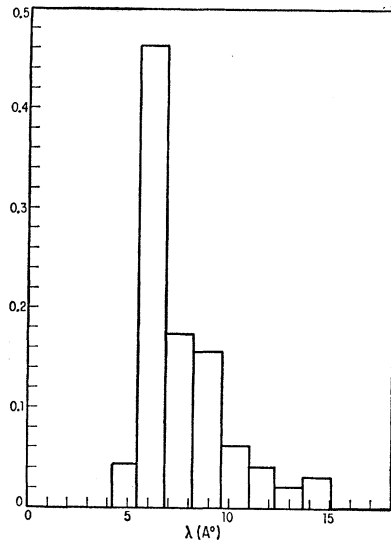


FIG. 8. Fractional contribution to the resistivity of sodium by phonon of wavelength λ . $T = 273^\circ\text{K}$.

We conclude from this small change that higher harmonics in the electron distribution contribute little to the resistivity. The reciprocal lattice is face-centered cubic and an electron in a state at any point in the zone is never very far from a symmetry (low phonon frequency) axis. Our calculations indicate that it would find no dearth of phonons with which to interact.

(ii) Phonon Drag

Equation (2.1) was calculated under the assumption that the phonons are in thermal equilibrium. But the presence of a current in the metal distorts the phonon distribution; if it is not brought to equilibrium in a time small compared with the phonon-electron mean collision time, the phonons will in turn drag the electrons along and lower the resistivity. This effect is most pronounced at low temperatures when the phonons interact primarily with electrons and the influence of other relaxation mechanisms is diminished. Sondheimer³⁰ has calculated this effect using the Debye theory of lattice vibrations and found it small. In view of this and the preponderance of umklapp processes we do not expect much of a phonon drag effect. Nevertheless, to obtain further empirical evidence on this point we have proposed an experiment.

If impurities are present in sufficient concentration, the phonons may be returned to equilibrium by collisions with impurities rapidly enough so that the elec-

TABLE II. Resistivity in $\mu\Omega$ cm calculated by use of trial functions (6.1).

$T(^{\circ}\text{K})$	ϕ_1	ϕ_2	ϕ_3	ϕ_4	ϕ_5	expt.
40	0.295	0.284	0.284	0.284	0.283	0.176
273	4.0	3.95	3.95	3.95	3.90	4.35

³⁰ E. H. Sondheimer, Can. J. Phys. **34**, 1246 (1956).

trons interact always with a thermal distribution of phonons. For this condition, we must have $\tau_{pi} < \tau_{pe}$, the average time for the collision of a phonon with an impurity must be smaller than that for a collision with an electron. The former interaction is governed by a Rayleigh-type scattering law³¹ so that $\tau_{pi} \sim \lambda^4$, where λ is the phonon wavelength. Since the most effective phonons are of short wavelength, a small amount of impurity might serve to equilibrate the phonons. Then the change in resistivity due to the addition of impurities will consist of a part due to the scattering of electrons from the impurity atoms themselves and a part due to decrease in phonon drag. The first part should be temperature-independent and should depend linearly on the concentration. The second part should have more complex dependence on the concentration and temperature and disappear altogether at concentrations and temperatures at which $\tau_{pi} \ll \tau_{pe}$. Thus we should observe a breakdown of Matthiessen's rule. An experiment to look for this effect is now being carried out.

(2) Liquid

Our calculations substantially overestimate the change in resistivity at the melting point and fail to predict the observed rapid increase with temperature in the liquid. The magnitude of the calculated resistivity then comes into fair agreement with experiment at 598°K . It seems clear from Fig. 3 that the neutron data themselves do not reflect the rapid change with temperature of the resistivity.

One possible explanation might have been that the static approximation fails for the slow-moving neutrons and hence the scattering data does not correctly picture the ionic configuration. To check this we have examined a higher order term in the expansion of ρ in the frequency moments of $S(\mathbf{q}, \omega)$.

From (2.2)

$$\rho = \frac{3}{16e^2 k_F^4 v_F^2} \int_{q < 2k_F} d^3 q q |f(\mathbf{q})|^2 \int d\omega S(\mathbf{q}, \omega) \frac{\beta\omega}{1 - e^{-\beta\omega}},$$

where

$$\beta = \hbar/kT.$$

Then, above the melting point,

$$\begin{aligned} \rho &= \frac{3}{16e^2 k_F^4 v_F^2} \int d^3 q q |f(\mathbf{q})|^2 \\ &\quad \times \int d\omega S(\mathbf{q}, \omega) [1 + (\beta\omega/2) + \dots] \\ &= \frac{3}{16e^2 k_F^4 v_F^2} \int d^3 q q |f(\mathbf{q})|^2 \\ &\quad \times \left[S^{(0)}(\mathbf{q}) + \frac{\beta}{2} S^{(1)}(\mathbf{q}) + \dots \right], \quad (7.1) \end{aligned}$$

where

$$S^{(n)}(\mathbf{q}) = \int d\omega S(\mathbf{q}, \omega) \omega^n.$$

³¹ P. G. Klemens, Solid State Phys. **7**, 18 (1958).

There is a sum rule, whose derivation depends on the potential being a function of particle coordinates only,³² which gives $S^{(1)}(\mathbf{q})$ immediately. It requires

$$S^{(1)}(\mathbf{q}) = \hbar q^2 / 2M, \quad (7.2)$$

where M is the ionic mass. So

$$\rho = \frac{3}{16e^2 k_F^4 v_F^2} \int_{q < 2k_F} d^3 q q |f(\mathbf{q})|^2 \times \left[S^{(0)}(q) + \frac{\hbar^2 q^2}{4MkT} + \dots \right]. \quad (7.3)$$

The second term was calculated using both f_A and f_B at 373 and 598°K and found to add less than 2% to the resistivity in all cases.

$S(\mathbf{q}, \omega)$ was recently measured and its moments computed for liquid sodium by Randolph.³³ He found that his $S^{(0)}(\mathbf{q})$ agreed with Gingrich and Heaton's results¹³ but found $S^{(1)}(\mathbf{q})$ to be two to three times greater than predicted theoretically by Eq. (7.2). This in itself would change our results little but it might be indicative of velocity-dependent forces in the liquid metal.

Alternatively it is conceivable that the electronic states undergo a significant change in going from the solid to the liquid phase. This would show up in a comparison of the additional resistivity induced by a fixed concentration of impurity atoms in the liquid with that in the solid. This also remains to be checked experimentally.

ACKNOWLEDGMENTS

We are very grateful for the many helpful discussions with Dr. L. Sham. We wish also to thank Professor S. Schultz for his active interest in the experimental aspects of this problem.

Notes added in proof.

1. Since this work was completed there has appeared a paper by A. Hasegawa³⁴ dealing with the same problem in the low and high temperature solid regimes. His results are qualitatively similar to ours although some of the numbers differ slightly.

2. In a recent paper Darby and March³⁵ (DM) report good agreement between their theoretical calculations for solid sodium from 15°K to 300°K and experiment. (Actually their theory should be compared with experimental data at constant pressure which at room temperature are about 20% higher than those quoted.) We wish here to clarify the relationship between their work and ours. Our calculation is in most respects more refined than that of DM; however DM include in an approximate way the change of the elastic constants

with temperature. This rather large effect (c_{44} changes by other 30%!) is a result of anharmonicities and was neglected in our paper along with all other anharmonic effects. When we incorporate the temperature dependence of the elastic constants into our calculation, we find that we can fit the experimental resistance over the entire temperature range to within about $\pm 20\%$. We find rather surprisingly that these anharmonic effects are already very important even at 150°K. What the importance of other anharmonic effects is we do not know. In any case it appears that a quantitative harmonic theory for Na is not possible.

Under these circumstances the following experimental information would be especially valuable: phonon frequencies measured at several temperatures, and a direct measurement of $S(q, \omega)$ for solid Na at several temperatures, which would include all anharmonic effects.

APPENDIX

The variational solution of the Boltzmann equation was obtained by Kohler³⁶ and Sondheimer²⁹ and is clearly set forth by Ziman³⁷ from whom we borrow the general formulation.

The variational expression for resistivity is

$$\rho = P/J^2, \quad (A1)$$

where

$$J = \int ev_{\mathbf{k}} \phi_{\mathbf{k}} \frac{\partial f_{\mathbf{k}}}{\partial E_{\mathbf{k}}} d^3 k \quad (A2)$$

and

$$P = (1/2kT) \iint [\phi_{\mathbf{k}} - \phi_{\mathbf{k}'}]^2 \pi(\mathbf{k}, \mathbf{k}') d^3 k d^3 k'. \quad (A3)$$

Here \mathbf{k} is the wave vector defining the one particle state, and $v_{\mathbf{k}}$ is the velocity and $E_{\mathbf{k}}$ the energy of that state. The probability of occupancy is given at equilibrium by the Fermi function $f_{\mathbf{k}} = \{\exp[(E_{\mathbf{k}} - E_F)/kT] + 1\}^{-1}$. $\phi_{\mathbf{k}}$ is a trial function, defining a perturbed distribution of the form $F(\mathbf{k}) = f_{\mathbf{k}} + \phi_{\mathbf{k}}(\partial f_{\mathbf{k}}/\partial E_{\mathbf{k}})$. We can see from (A2) that J represents the current carried by the function $F(\mathbf{k})$, while P is related to the rate of return of the system to equilibrium when $\pi(\mathbf{k}, \mathbf{k}')$ is the total probability that an electron is in state \mathbf{k} and is scattered to state \mathbf{k}' . The variational principle states that $\phi_{\mathbf{k}}$ must be chosen to make ρ of Eq. (A1) a minimum.

From time-dependent perturbation theory

$$\pi(\mathbf{k}, \mathbf{k}') = (2\pi/\hbar) |M(\mathbf{k}, \mathbf{k}')|^2 \times f_{\mathbf{k}}(1 - f_{\mathbf{k}'}) \delta(E_{\mathbf{k}} - E_{\mathbf{k}'} + \hbar\omega). \quad (A4)$$

According to Van Hove,¹⁰ in the weak-scattering case we can write this

$$\pi(\mathbf{k}, \mathbf{k}') = (2\pi/\hbar) |f(\mathbf{q})|^2 f_{\mathbf{k}}(1 - f_{\mathbf{k}'}),$$

where $\mathbf{q} = \mathbf{k}' - \mathbf{k}$, $f(\mathbf{q})$ is the scattering amplitude, and

³² A. Rahman, K. S. Singwi, and A. Sjölander, Phys. Rev. **126**, 986 (1962).

³³ P. D. Randolph, Phys. Rev. **134**, A1238 (1964).

³⁴ A. Hasegawa, J. Phys. Soc. Japan **19**, 504 (1964).

³⁵ J. K. Darby and N. H. March, Proc. Phys. Soc. (London) **84**, 591 (1964).

³⁶ M. Kohler, Z. Physik **125**, 679 (1949).

³⁷ J. Ziman, *Electrons and Phonons* (Oxford University Press, New York, 1960), Chap. 9.

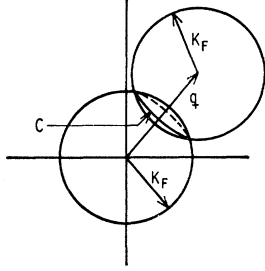


FIG. 9. Path of integration C for $\oint d^3k$.

$S(\mathbf{q}, \omega)$ is the spectral function

$$S(\mathbf{q}, \omega) = \int \frac{dt}{2\pi N} e^{-i\omega t} \left\langle \sum_{i,j=1}^N e^{-i\mathbf{q} \cdot \mathbf{r}_i(0)} e^{i\mathbf{q} \cdot \mathbf{r}_j(t)} \right\rangle_T.$$

Then

$$P = \frac{2\pi}{2\hbar k T} \int \int d^3k d^3k' [\phi_{\mathbf{k}} - \phi_{\mathbf{k}'}]^2 |f(\mathbf{q})|^2 \times f_{\mathbf{k}}(1 - f_{\mathbf{k}'}) S(\mathbf{q}, \omega). \quad (\text{A5})$$

Now, letting $\mathcal{E}_{\mathbf{k}} = E_{\mathbf{k}} - E_F$ (E_F is the Fermi energy), we have

$$\begin{aligned} \int d^3k' &= \int \frac{d\mathcal{E}_{\mathbf{k}'}}{8\pi^3 \hbar v_{\mathbf{k}'}} \int d^2S_{\mathbf{k}'} \\ &= \int (\hbar\omega / 8\pi^3 v_{\mathbf{k}'}) \int_{\text{F.S.}} d^2S_{\mathbf{k}'}, \end{aligned}$$

where $\hbar\omega = \mathcal{E}_{\mathbf{k}'} - \mathcal{E}_{\mathbf{k}}$ and the surface integral can be taken on the Fermi surface when $\hbar\omega \ll E_F$.

$$\begin{aligned} &\int d^3k f_{\mathbf{k}}(1 - f_{\mathbf{k}'}) \\ &= \int \frac{d\mathcal{E}_{\mathbf{k}}}{4\pi^3 v_{\mathbf{k}} \hbar} \frac{1}{((e^{\mathcal{E}_{\mathbf{k}}/kT} + 1)(1 + e^{-(\mathcal{E}_{\mathbf{k}} + \hbar\omega)/kT}))} \int d^2S_{\mathbf{k}} \\ &= (1/4\pi^3 \hbar v_{\mathbf{k}}) \hbar\omega / (1 - e^{-\hbar\omega/kT}) \int_{\text{F.S.}} d^2S_{\mathbf{k}}. \end{aligned}$$

Then

$$\begin{aligned} P &= (\pi/kT)(1/32\pi^6) \int \int_{\text{F.S.}} (d^2S_{\mathbf{k}'}/\hbar v_{\mathbf{k}'}) d^2S_{\mathbf{k}} [\phi_{\mathbf{k}} - \phi_{\mathbf{k}'}]^2 \\ &\quad \times |f(\mathbf{q})|^2 \int d\omega S(\mathbf{q}, \omega) \omega / (1 - e^{-\hbar\omega/kT}). \quad (\text{A6}) \end{aligned}$$

Now

$$\begin{aligned} \int \int_{\text{F.S.}} d^2S_{\mathbf{k}} d^2S_{\mathbf{k}'} &= \int d^3k \int d^3k' \delta(k - k_F) \delta(k' - k_F) \\ &= \int d^3k \int d^3q \delta(k - k_F) \delta(|\mathbf{k} + \mathbf{q}| - k_F) \\ &= \int_{q < 2k_F} d^3q \oint dk, \end{aligned}$$

where we have written

$$\oint dk = \int d^3k \delta(k - k_F) \delta(|\mathbf{k} + \mathbf{q}| - k_F).$$

The two delta functions each define a sphere of radius k_F and the two spheres are displaced by a distance \mathbf{q} .

The integral $\oint dk$ is a line integral around the circle which represents the intersection of the two spheres; we define it to be zero when $q > 2k_F$. See Fig. 9. Then

$$P = (\hbar^2 32\pi^6 v_{\mathbf{k}}^2)^{-1} \int_{q < 2k_F} d^3q \oint dk [\phi_{\mathbf{k}} - \phi_{\mathbf{k}'}]^2 |f(\mathbf{q})|^2 \times \int d\omega S(\mathbf{q}, \omega) \frac{\beta\omega}{(1 - e^{-\beta\omega})}. \quad (\text{A7})$$

For the special case where $\phi_{\mathbf{k}} - \phi_{\mathbf{k}'}$ is a function of \mathbf{q} alone we have

$$P = (16\pi^4 \hbar^2 v_{\mathbf{k}}^2)^{-1} k_F^2 \int \frac{d^3q}{q} [\phi_{\mathbf{k}} - \phi_{\mathbf{k}'}]^2 |f(\mathbf{q})|^2 \mathcal{S}(\mathbf{q}), \quad (\text{A8})$$

where, as in the text,

$$\mathcal{S}(\mathbf{q}) = \frac{\hbar}{kT} \int d\omega S(\mathbf{q}, \omega) \frac{\omega}{1 - e^{-\beta\omega}}. \quad (\text{A9})$$

Assume an electric field in the z direction. We must choose a trial function which changes sign when $z \rightarrow -z$ but otherwise exhibits cubic symmetry. When the scattering is elastic, i.e., $S(\mathbf{q}, \omega) \sim \delta(\omega)$, the simplest such function $\phi_{\mathbf{k}} = k_z$ provides an exact solution of the Boltzmann equation. For phonon scattering, where $\hbar\omega$ is always much less than E_F , we have nearly elastic scattering from the point of view of the electrons and so we may try the same function. Using (A8) we get

$$P = (16\pi^4 \hbar^2 v_{\mathbf{k}}^2)^{-1} k_F^2 \int_{q < 2k_F} (d^3q/q) q_z^2 |f(\mathbf{q})|^2 \mathcal{S}(\mathbf{q}). \quad (\text{A10})$$

Using this function in (A2)

$$J = (k_F^3/3\pi^2)(e/\hbar),$$

and finally, taking account of cubic symmetry, we have

$$\rho = \frac{3}{16e^2 v_{\mathbf{k}}^2 k_F^4} \int_{q < 2k_F} d^3q q |f(\mathbf{q})|^2 \mathcal{S}(\mathbf{q}), \quad (\text{A11})$$

with $\mathcal{S}(\mathbf{q})$ defined by (A9).

To use a more complex trial function, we expand $\phi_{\mathbf{k}}$ in the form

$$\phi_{\mathbf{k}} = \sum_i a_i \phi_{\mathbf{k}}^{(i)},$$

where $\phi_{\mathbf{k}}^{(i)}$ are a finite set of appropriate functions. We must insert this in (A1) and minimize ρ with respect to the coefficients a_i . So doing, we obtain³⁸

$$(1/\rho) = \sum_{ij} J_i (P^{-1})_{ij} J_j,$$

where

$$J_i = \int e \mathbf{v}_{\mathbf{k}} \phi_{\mathbf{k}}^{(i)} \frac{\partial f_{\mathbf{k}}}{\partial \mathcal{E}_{\mathbf{k}}} d^3k,$$

$$P_{ij} = (32\pi^5 \hbar^2 v_{\mathbf{k}}^2)^{-1} \int d^3q \oint dk [\phi_{\mathbf{k}}^{(i)} - \phi_{\mathbf{k}'}^{(i)}] \times [\phi_{\mathbf{k}}^{(j)} - \phi_{\mathbf{k}'}^{(j)}] |f(\mathbf{q})|^2 \mathcal{S}(\mathbf{q}),$$

and P^{-1} is the inverse of the matrix $\{P_{ij}\}$.

³⁸ See Ref. 37, p. 285.